

## Avoided Level Crossing Muon Spectroscopy of Free Radicals Formed by Muonium Addition to the Constituents of DNA

Penny L. Hubbard,<sup>†</sup> Vasily S. Oganessian,<sup>†,‡</sup> Nail Sulaimanov,<sup>‡</sup> Julea N. Butt,<sup>†,‡,§</sup> and Upali A. Jayasooriya<sup>\*,†</sup>

*School of Chemical Sciences and Pharmacy, Centre for Metalloprotein Spectroscopy and Biology, and School of Biological Sciences, University of East Anglia, Norwich NR4 7TJ, United Kingdom, and Paul Scherrer Institute, Villigen, Switzerland*

*Received: June 8, 2004; In Final Form: July 27, 2004*

Avoided level crossing muon spectra (ALC- $\mu$ SR) of the free radicals formed by muonium addition to nucleic acid bases adenine, cytosine, guanine, thymine, and uracil are reported and assigned by using ab initio DFT calculations. The following radicals and their hyperfine constants,  $A_{\mu}$ , were identified: adenine, C<sub>8</sub> (the radical formed by adding Mu to the C<sub>8</sub> carbon of adenine) = 424.1 MHz; cytosine, C<sub>5</sub> = 406.1 MHz and C<sub>6</sub> = 593.0 MHz; guanine, C<sub>5</sub> = 657.1 MHz and C<sub>8</sub> = 407.5 MHz; thymine, C<sub>5</sub> = 494.3 MHz and O<sub>2</sub> = 409.7 MHz; and uracil, C<sub>5</sub> = 381.7 MHz, C<sub>6</sub> = 553.6 MHz, O<sub>2</sub> = 418.1 MHz, and O<sub>4</sub> = 149.7 MHz. No ALC- $\mu$ SR resonances were observed from polycrystalline samples of the sugar ribose or potassium phosphate at 300 K. Preliminary ALC- $\mu$ SR spectra of a double stranded (ds) DNA sample are reported and found to show additional resonances to those of the nucleic acid bases, indicating the behavior of implanted muons in dsDNA to be more complex than a simple sum of the behaviors found with the bases. The reported data are also pertinent to H atom adducts of these materials, where the hyperfine parameters are scaled by the ratio of the gyromagnetic ratio of the muon to that of the proton.

### Introduction

Several reports have appeared in the literature showing the possibility of using muon spectroscopies to study the properties of DNA.<sup>1,2</sup> Muon spin relaxation studies with DNA and related materials have shown distinct differences in the behavior of double stranded DNA (dsDNA) compared to single stranded DNA (ssDNA) and the free nucleic acid bases.<sup>1</sup> The sensitivity of the relaxation of the implanted muons to the secondary structure of dsDNA has been illustrated by comparing the A and B forms.<sup>2</sup> It should be possible to extract much more microscopic information about DNA from muon spectroscopies, including properties such as those associated with excess electron conduction. This is because of the inherent nature of the muon implantation studies where the implanted muon picks up an electron to form muonium, a lighter isotope of hydrogen, which then adds to unsaturated centers such as double bonds in the parent molecule. The properties of the resulting radical electron are then monitored by the muon to convey the properties of the radical species. However, the reliability of the estimates of such properties will clearly depend on the accurate measurement of the hyperfine parameters.<sup>3</sup> It is therefore important to have a detailed understanding of the sites of muonium addition to DNA if the advantages of  $\mu$ SR are to be fully exploited for DNA investigations. The questions that need answers include the following: Which of the possible muonium addition sites in the constituents of DNA, i.e., the bases, sugar ribose, and the phosphate group, are populated and what are their hyperfine parameters? Are the sites favored by muonium

on addition to DNA identical to those found with isolated individual bases, and if so are the hyperfine parameters the same as in the case of an isolated constituent? Finally what possibilities are there of monitoring these sites individually when within the DNA molecule?

Muon implantation to produce radical species from unsaturated organic compounds is well established.<sup>4</sup> The acronym  $\mu$ SR stands for muon spin rotation, relaxation, and resonance covering the various ways in which the evolution of the muon polarization is studied. Detection and characterization of radical species with exceptional sensitivity is now possible by using spin-polarized muons and single-particle counting techniques.<sup>4</sup> Similar to conventional magnetic resonance, characteristic frequencies provide measurements of internal magnetic or hyperfine parameters. The muon spin plays the role of a nuclear spin, but the spectroscopy proves to be equally sensitive both to muons in electronically diamagnetic environments and to those which experience a hyperfine coupling with paramagnetic electrons, the latter being of importance to the studies involving organic radicals. The chemical reactions of muonium mimic those of atomic hydrogen and form the basis of muonium chemistry. The main interaction that is observed in a muoniated radical species is that between the muon and the unpaired electron created by the muonium addition process. The most direct way to measure the hyperfine frequencies is by muon spin rotation experiments in a transverse magnetic field (TF- $\mu$ SR). Use of single crystals with this technique provides the most detailed information on this interaction. This method is also applicable to the liquid/solution state, where the isotropic part of this interaction is measured. Solution state spectroscopy with transverse magnetic fields requires prompt addition of muonium, within about a nanosecond to create the molecule of interest, to observe the resulting radical before the polarization information is lost. Hence there is the need for highly concentrated

\* To whom correspondence should be addressed. Fax +44 (0) 1603 592003. E-mail: u.jayasooriya@uea.ac.uk.

<sup>†</sup> School of Chemical Sciences and Pharmacy, University of East Anglia.

<sup>‡</sup> Centre for Metalloprotein Spectroscopy and Biology, University of East Anglia.

<sup>§</sup> School of Biological Sciences, University of East Anglia.

<sup>‡</sup> Paul Scherrer Institute.

solutions. It was not possible to make large enough single crystals, stable melts, or solutions of high enough solubility in a suitable solvent of the nucleic acid bases investigated in this report for TF- $\mu$ SR to be applicable. Under such conditions, measurements of the hyperfine interactions can be made by using longitudinal field (LF) experiments. LF-relaxation measurements provide only an approximate value of the hyperfine interaction while the measurement of "polarization dips" due to the high field level crossing resonances provides more accurate values of this interaction. The latter technique has the great advantage of being applicable to even powder or polycrystalline samples, and is the method used in the measurements reported in this paper. Barnabas et al.<sup>5</sup> have applied this technique to study the bases uracil and thymine in solution state, where the level crossing resonance signals are confined to those observable under isotropic conditions only. Use of solid samples as done in the present study gives access to a wider range of resonances.<sup>4</sup>

To carry out a systematic investigation of the nucleic acid bases, we have performed ab initio DFT calculations for all possible radical species that are expected from muonium addition to each base, and estimated their structural and hyperfine parameters. Some of these results are already published, where a surprise finding was the exceptionally large hyperfine interactions for muonium addition to the oxygen atoms of C=O bonds in several of these ring compounds.<sup>6</sup> Here we report the experimental measurements and assignments of the radicals formed by all these bases using avoided-level-crossing  $\mu$ SR (ALC- $\mu$ SR) spectroscopy. ALC- $\mu$ SR spectra of a powder sample of dsDNA are also reported and discussed with a comparison of the resonances to those of individual bases.

## Experimental Section

Samples of the nucleic acid bases, adenine, cytosine, guanine, thymine, and uracil, and potassium phosphate and the sugar ribose were purchased from Sigma-Aldrich and Avacado companies and used without further purification. Herring tested dsDNA samples were purchased from Sigma-Aldrich and further purified using standard methods to remove any traces of proteins present.

**Spectroscopy.** Time integral longitudinal field  $\mu$ SR measurements were made of powder samples, ca. 4 cm in diameter and 3 mm thick, mounted on a copper backing plate and covered with a thin Mylar film sealed in place with a copper ring plate. The ALC spectrometer setup in the  $\pi$ E3 beam at the Paul Scherrer Institute, Switzerland, (PSI), was used.<sup>4</sup> Spectra were also run with polycrystalline samples of potassium phosphate and the sugar ribose. These two samples did not show any detectable resonances within the field range 0.001 to 5 T, and therefore these scans were used as suitable background spectra for spectral subtraction.

**Ab Initio DFT Computational Details.** The calculations described in this work were performed on a Linux/Pentium III based workstation with use of the Amsterdam Density Functional (ADF) program, version 2000.0.1.<sup>7</sup> The local exchange-correlation approximation (LDA) of Vosko, Wilk, and Nusair<sup>8</sup> was used. The final results show that this level of approximation gives predictions of the desired physical quantities with sufficient accuracy for these molecules. Inclusion of the nonlocal gradient corrections of Becke<sup>9</sup> for exchange, and Perdew<sup>10</sup> for correlation, changes the calculated values of hyperfine couplings only slightly (<10%). All molecular calculations were of spin-unrestricted type, so as to allow for substantial spin-polarization on atoms. An uncontracted triple- $\zeta$  basis set (ADF basis set IV) with a single set of polarization functions was used for all

atoms. In particular, carbon atoms were modeled with triple- $\zeta$  2s, 2p, and one 3d polarization function and hydrogen and muonium atoms were with triple- $\zeta$  1s and one 2p polarization function. All geometry optimizations were performed, at the same level of theory, using the algorithm of Versluis and Zeigler.<sup>11</sup> Starting geometries were calculated by using Molecular Mechanics (MM) force field methods.<sup>12</sup>

## Results

The experimentally measured longitudinal field time integral (ALC) spectra of the individual nucleic acid bases are reported followed by a summary of results from the ab initio DFT calculations. Good correlations were found between theoretical predictions and experimental observations thus providing a method of unambiguous assignment of the observed resonances. This also provides a final scaling of the theoretical values. Spectra of a solid sample of dsDNA are also reported and discussed.

**Longitudinal-Field Avoided Level Crossing (ALC- $\mu$ SR) Measurements.** The experimentally observed longitudinal field time integral measured (ALC) spectra of the nucleic acid bases, adenine, cytosine, guanine, thymine, and uracil, after appropriate background subtractions, are shown in Figures 1 to 3 as derivative spectra. The experimentally observed resonance fields estimated by comparing these derivative spectra with the raw spectral information on ALC "polarization dips" for all measured temperatures are given in Table 1. A complete data set from all the bases are available only at a sample temperature of 300 K, and therefore this data set was used for the search for correlations that are discussed later. The labeling scheme of the nucleic acid bases that is used in this paper is shown in Figure 4.

The ab initio DFT calculated hyperfine interactions for muonium addition to all possible centers in these nucleic acid bases are summarized in Table 2. All hyperfine tensors were found to have approximate axial symmetry. Some of this theoretical information was presented in an earlier publication.<sup>6</sup>

**Comparison between Theory and Experiment.** For an excellent review and details of the ALC- $\mu$ SR technique see Roduner.<sup>4</sup> In high magnetic fields, the spin eigenstates are good approximations to pure Zeeman states and thus their energies vary linearly with the applied magnetic field. These states may then truly cross in an energy-field diagram. However, if these levels have either an off-diagonal element in the energy matrix, as written in the conventional Zeeman basis, which mixes the two states directly, or they mix indirectly via coupling of both states to a common, energetically remote state, then these states instead of crossing would avoid each other. The following three conditions must then be obeyed for the effects of this avoidance to be observed in longitudinal-field  $\mu$ SR experiments. First there must be an element in the Hamiltonian that leads to a mixing of these states, and then this element must be sufficiently large to cause a minimum separation,  $\Delta E$ , of the levels so that the oscillation between the states occurs with a frequency  $\nu_r$ , or in a time  $\nu_r^{-1} = h/\Delta E$ , which is short or comparable to the muon lifetime, and finally, one of the eigenstates must have the muon spin "up" and the other one muon spin "down". The signals thus observed are called avoided level crossing resonances (ALC), and sometime these are also referred to as anticrossing resonances or simply as level crossing resonances. There are three selection rules for the observation of ALC resonances where the total spin quantum number,  $M$ , can either change by 0, 1, or 2 units.  $|\Delta M| = 1$  corresponds to a transition where only the muon spin flips.  $|\Delta M| = 0$  corresponds to the situation

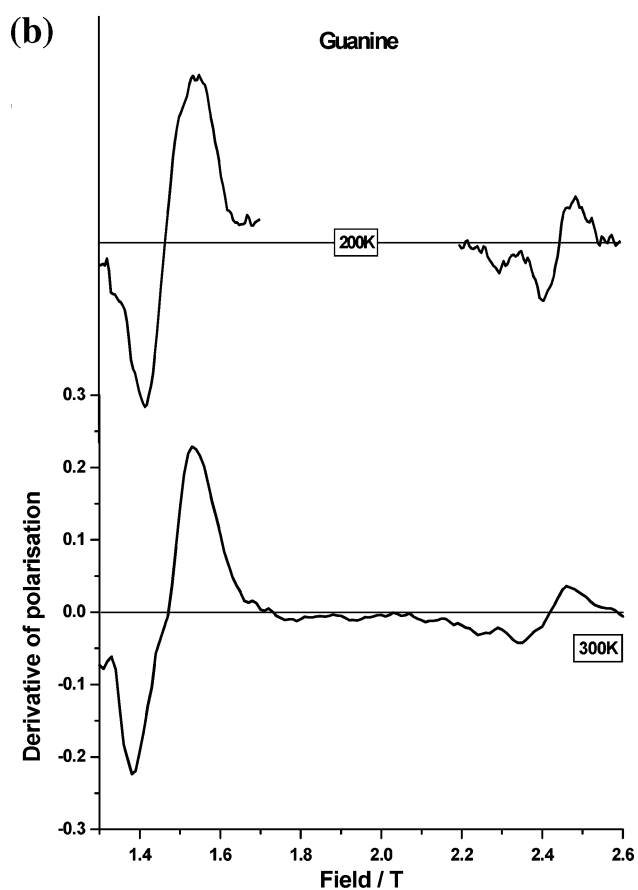
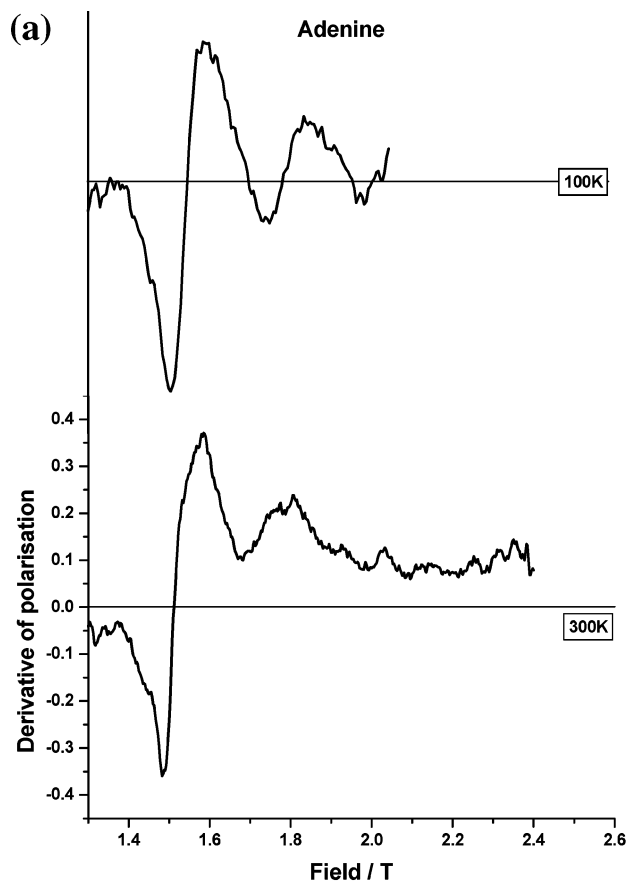


**Figure 1.** ALC spectra of polycrystalline samples of the purine bases (a) adenine and (b) guanine at the highest and lowest temperatures studied for each sample. Gaps in the spectra show the regions where experimental data were not collected.

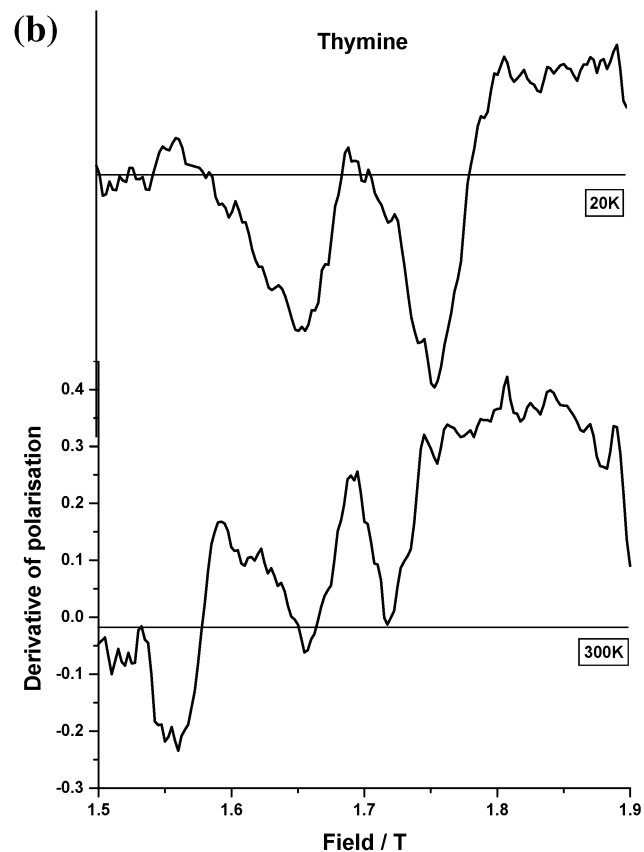
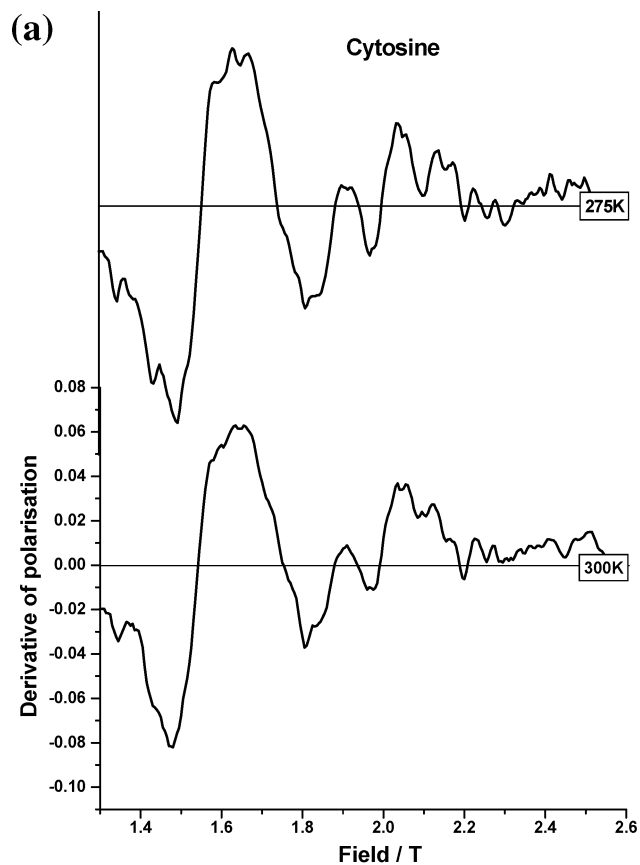


**Figure 2.** ALC spectra of polycrystalline samples of the pyrimidine bases (a) cytosine and (b) thymine at the highest and lowest temperatures studied for each sample.

where another spin  $1/2$  nucleus such as that of a hydrogen atom is also involved. The latter would then be a muon–proton spin

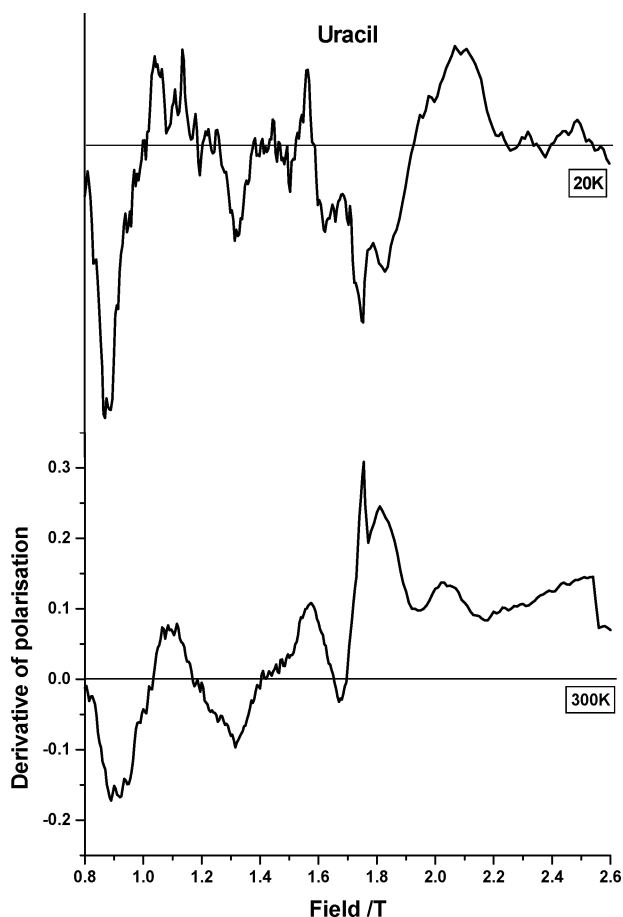


**Figure 3.** ALC spectra of polycrystalline samples of uracil at the highest and lowest temperatures studied for each sample.

**TABLE 1: Experimentally Observed ALC Resonances of the Nucleic Acid Bases at Different Temperatures**

compd	obsd resonances/T					
	20 K	100 K	200 K	250 K	275 K	300 K
adenine		1.540	1.525	1.520		1.507
			1.780	1.775	1.750	1.730
cytosine		2.000	2.000	2.000	1.537	1.532
					1.892	1.870
guanine			1.464	1.455	1.459	1.450
			2.445	2.430	2.420	2.407
thymine	1.682	1.661	1.627			1.580
	1.720	1.690				1.665
uracil	1.78	1.765	1.754			1.724
	0.980	0.974	0.968			1.037
	1.367	1.361	1.400			1.400
	1.540	1.537	1.530			1.530
	1.840	1.830	1.790			1.706
	2.105	2.021	2.000			1.952
	2.290	2.270	2.230			2.170

flip-flop transition.  $|\Delta M| = 2$  gives a very much weaker and sharper signal, and it is due to a transition consisting of muon-proton spin flip-flip. The latter transitions are not often observed.

The fields at which the level crossing resonances are expected from the ab initio DFT calculated hyperfine interactions were estimated following the detailed theoretical treatment given by Heming et al.<sup>13</sup>

For the  $|\Delta M| = 0$  transition the field ( $B_0$ ) at which the ALC occurs is given by the following equation

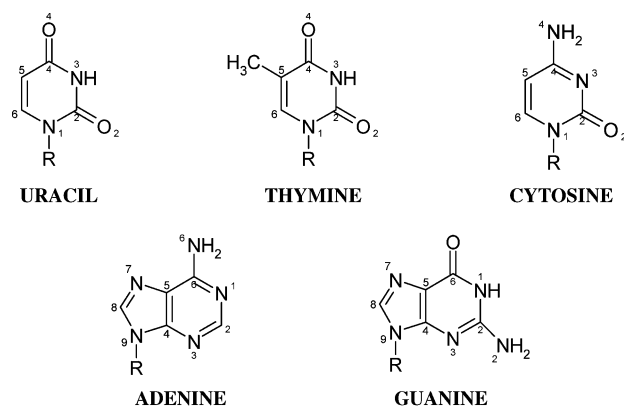


**Figure 4.** Structures of the bases together with the numbering scheme used in this paper.

**TABLE 2: Ab Initio Calculated Hyperfine Coupling Parameters for All Possible Muon Adducts of the Nucleic Acid Bases**

unsaturated center	muon addition	isotropic $A_{\mu}/\text{MHz}$	anisotropic $A_{\mu\parallel}/\text{MHz}$	anisotropic $A_{\mu\perp}/\text{MHz}$	$e^-$ density ( $\mu$ 1s)
adenine (with N-CH <sub>3</sub> )					
C <sub>2</sub> =N <sub>3</sub>	C <sub>2</sub>	515.5	533.3	506.55	
C <sub>2</sub> =N <sub>3</sub>	N <sub>3</sub>	-32.3	4.7	-50.85	
C <sub>6</sub> =N <sub>1</sub>	N <sub>1</sub>	4.0	10.1	1.0	
C <sub>6</sub> =N <sub>1</sub>	C <sub>6</sub>	712.1	724.4	705.9	
C <sub>4</sub> =C <sub>5</sub>	C <sub>5</sub>	587.7	594.0	584.6	
C <sub>4</sub> =C <sub>5</sub>	C <sub>4</sub>	725.5	735.9	720.35	
C <sub>8</sub> =N <sub>7</sub>	C <sub>8</sub>	404.3	418.5	397.15	
C <sub>8</sub> =N <sub>7</sub>	N <sub>7</sub>	82.2	125.0	60.85	
cytosine (with N-CH <sub>3</sub> )					
C <sub>2</sub> =O <sub>2</sub>	C <sub>2</sub>	1850.0	1871.4	1839.25	
C <sub>2</sub> =O <sub>2</sub>	O <sub>2</sub>	-1.1	8.2	-5.7	<1.0%
C <sub>4</sub> =N <sub>3</sub>	C <sub>4</sub>	1483.5	1508.5	1470.95	
C <sub>4</sub> =N <sub>3</sub>	N <sub>3</sub>	-27.5	-0.03	-41.3	
C <sub>5</sub> =C <sub>6</sub>	C <sub>5</sub>	392.2	413.7	381.4	
C <sub>5</sub> =C <sub>6</sub>	C <sub>6</sub>	533.9	554.5	523.6	
guanine (with N-CH <sub>3</sub> )					
C <sub>2</sub> =N <sub>3</sub>	C <sub>2</sub>	426.8	441.3	419.55	
C <sub>2</sub> =N <sub>3</sub>	N <sub>3</sub>	-19.2	18.0	-37.8	
C <sub>6</sub> =O <sub>6</sub>	C <sub>6</sub>	69.3	88.0	59.9	
C <sub>6</sub> =O <sub>6</sub>	O <sub>6</sub>	-11.1	20.9	-27.15	<1.0%
C <sub>5</sub> =C <sub>4</sub>	C <sub>5</sub>	579.8	588.3	575.5	
C <sub>5</sub> =C <sub>4</sub>	C <sub>4</sub>	494.3	506.2	488.4	
C <sub>8</sub> =N <sub>7</sub>	C <sub>8</sub>	391.8	406.7	384.4	
C <sub>8</sub> =N <sub>7</sub>	N <sub>7</sub>	-52.5	1.43	-79.45	
thymine (with N-CH <sub>3</sub> )					
C <sub>2</sub> =O <sub>2</sub>	C <sub>2</sub>	1285.8	1300.6	1278.35	
C <sub>2</sub> =O <sub>2</sub>	O <sub>2</sub>	394.2	412.4	385.05	13.0%
C <sub>4</sub> =O <sub>4</sub>	C <sub>4</sub>	36.9	57.2	26.8	
C <sub>4</sub> =O <sub>4</sub>	O <sub>4</sub>	192.1	210.2	183.0	3.8%
C <sub>5</sub> =C <sub>6</sub>	C <sub>5</sub>	459.1	480.2	448.55	
C <sub>5</sub> =C <sub>6</sub>	C <sub>6</sub>	373.9	396.2	362.8	
uracil (with N-CH <sub>3</sub> )					
C <sub>2</sub> =O <sub>2</sub>	C <sub>2</sub>	1464.2	1492.6	1450.0	
C <sub>2</sub> =O <sub>2</sub>	O <sub>2</sub>	401.3	421.9	391.0	12.0%
C <sub>4</sub> =O <sub>4</sub>	C <sub>4</sub>	33.2	55.0	22.25	
C <sub>4</sub> =O <sub>4</sub>	O <sub>4</sub>	197.0	216.0	187.4	3.7%
C <sub>5</sub> =C <sub>6</sub>	C <sub>5</sub>	374.0	396.5	362.7	
C <sub>5</sub> =C <sub>6</sub>	C <sub>6</sub>	503.2	523.8	492.85	

$$B_0 = \left| \frac{A_{\mu} - A_p}{2(\gamma_{\mu} - \gamma_p)} - \frac{A_{\mu}^2 - 2MA_p^2}{2\gamma_c(A_{\mu} - A_p)} \right| \quad (1)$$

and for the  $|\Delta M| = 1$  transition

$$B_1 = [A_{\mu} + D_{\perp}(3 \cos^2 \theta - 1)] \left[ \frac{1}{2\gamma_{\mu}} - \frac{1}{2\gamma_c} \right] \quad (2)$$

**TABLE 3: Theoretically Predicted  $|\Delta M| = 1$  ALC Resonances for the Nucleic Acid Bases. Couplings Less than 10 MHz Are Not Included, out of Plane Angle of the Muon Position in the Case of the O-Mu Bonds Are Indicated in Paranthesis**

unsaturated center	muon addition site	$\Delta M = 1/T$ (estimated from ab initio calcs)
adenine (with N-CH <sub>3</sub> )		
C <sub>2</sub> =N <sub>3</sub>	C <sub>2</sub>	1.827–1.924
C <sub>2</sub> =N <sub>3</sub>	N <sub>3</sub>	~0
C <sub>6</sub> =N <sub>1</sub>	N <sub>1</sub>	~0
C <sub>6</sub> =N <sub>1</sub>	C <sub>6</sub>	2.568–2.635
C <sub>4</sub> =C <sub>5</sub>	C <sub>5</sub>	2.134–2.168
C <sub>4</sub> =C <sub>5</sub>	C <sub>4</sub>	2.624–2.682
C <sub>8</sub> =N <sub>7</sub>	C <sub>8</sub>	1.432–1.509
C <sub>8</sub> =N <sub>7</sub>	N <sub>7</sub>	0.145–0.381
cytosine (with N-CH <sub>3</sub> )		
C <sub>2</sub> =O <sub>2</sub>	C <sub>2</sub>	6.710–6.830
C <sub>2</sub> =O <sub>2</sub>	O <sub>2</sub> (35.7°)	~0
C <sub>4</sub> =N <sub>3</sub>	C <sub>4</sub>	5.353–5.490
C <sub>4</sub> =N <sub>3</sub>	N <sub>3</sub>	~0
C <sub>5</sub> =C <sub>6</sub>	C <sub>5</sub>	1.359–1.480
C <sub>5</sub> =C <sub>6</sub>	C <sub>6</sub>	1.883–1.998
guanine (with N-CH <sub>3</sub> )		
C <sub>2</sub> =N <sub>3</sub>	C <sub>2</sub>	1.514–1.592
C <sub>2</sub> =N <sub>3</sub>	N <sub>3</sub>	~0
C <sub>6</sub> =O <sub>6</sub>	C <sub>6</sub>	0.185–0.289
C <sub>6</sub> =O <sub>6</sub>	O <sub>6</sub> (9.0°)	~0
C <sub>5</sub> =C <sub>4</sub>	C <sub>5</sub>	2.097–2.143
C <sub>5</sub> =C <sub>4</sub>	C <sub>4</sub>	1.770–1.836
C <sub>8</sub> =N <sub>7</sub>	C <sub>8</sub>	1.384–1.464
C <sub>8</sub> =N <sub>7</sub>	N <sub>7</sub>	~0
thymine (with N-CH <sub>3</sub> )		
C <sub>2</sub> =O <sub>2</sub>	C <sub>2</sub>	4.665–4.745
C <sub>2</sub> =O <sub>2</sub>	O <sub>2</sub> (39.5°)	1.379–1.481
C <sub>4</sub> =O <sub>4</sub>	C <sub>4</sub>	0.062–0.172
C <sub>4</sub> =O <sub>4</sub>	O <sub>4</sub> (11.3°)	0.638–0.738
C <sub>5</sub> =C <sub>6</sub>	C <sub>5</sub>	1.607–1.724
C <sub>5</sub> =C <sub>6</sub>	C <sub>6</sub>	1.290–1.414
uracil (with N-CH <sub>3</sub> )		
C <sub>2</sub> =O <sub>2</sub>	C <sub>2</sub>	5.285–5.394
C <sub>2</sub> =O <sub>2</sub>	O <sub>2</sub> (30.2°)	1.398–1.508
C <sub>4</sub> =O <sub>4</sub>	C <sub>4</sub>	0.041–1.627
C <sub>4</sub> =O <sub>4</sub>	O <sub>4</sub> (9.0°)	0.653–0.758
C <sub>5</sub> =C <sub>6</sub>	C <sub>5</sub>	1.290–1.414
C <sub>5</sub> =C <sub>6</sub>	C <sub>6</sub>	1.765–1.897

where  $A_\mu$  and  $A_p$  are the hyperfine interactions of the muon and the proton,  $\gamma_\mu$  and  $\gamma_p$  are their magnetogyric ratios,  $D_\zeta$  is the hyperfine anisotropy defined as the difference between the isotropic and anisotropic coupling constants ( $A_\zeta - A_\mu$ ),  $\theta$  is the angle between the field direction and the Z axis of the hyperfine coupling tensor, and  $M$  is a quantum number.

Field spreads at which the  $|\Delta M| = 1$  resonances are predicted are given in Table 3. The ab initio estimated values of the hyperfine interactions with the closest protons in the radicals together with the calculated values for the  $|\Delta M| = 0$  resonances are given in Table 4.

The calculations performed were for isolated molecules while the experimental data are for solid state samples. Therefore it is reasonable to expect deviations between these two sets of values dependent on the solid state effects. This is indeed the case. Therefore it is not possible simply to relate experimental values to theory by a direct comparison of the individual values. However, as illustrated below, it is possible to arrive at satisfactory assignments by a comparison of all the experimental and theoretical values with use of linear correlations.

The search for correlation was made by first plotting the experimentally observed resonances against the closest calcu-

**TABLE 4: Theoretically Predicted  $|\Delta M| = 0$  ALC Resonances**

unsaturated center	muon addition	$A_\mu/\text{MHz}$	$A_p/\text{MHz}$	$\Delta M = 0/T$ (estimated from ab initio calcs)
adenine (with N-CH <sub>3</sub> )				
C <sub>5</sub> =C <sub>4</sub>	C <sub>5</sub>	587.6	-32 (H $\gamma$ )	3.325
C <sub>5</sub> =C <sub>4</sub>	C <sub>4</sub>	725.6	-14 (H $\gamma$ )	3.968
C <sub>2</sub> =N <sub>3</sub>	C <sub>2</sub>	515.4	160 (H $\alpha$ )	1.901
		515.4	-19 (H $\gamma$ )	2.867
C <sub>2</sub> =N <sub>3</sub>	N <sub>3</sub>	-32.1	-37 (H $\beta$ )	0.028
		-32.1	-16 (H $\gamma$ )	-0.086
C <sub>6</sub> =N <sub>1</sub>	C <sub>6</sub>	712	-19 (H $\beta$ )	3.922
C <sub>6</sub> =N <sub>1</sub>	N <sub>1</sub>	4.0	-24 (H $\beta$ )	0.016
		4.0	-22 (H $\gamma$ )	0.140
C <sub>8</sub> =N <sub>7</sub>	C <sub>8</sub>	404.1	121 (H $\alpha$ )	1.514
		404.1	-15 (H $\gamma$ )	2.249
C <sub>8</sub> =N <sub>7</sub>	N <sub>7</sub>	82.3	-58 (H $\beta$ )	0.755
cytosine (with N-CH <sub>3</sub> )				
C <sub>5</sub> =C <sub>6</sub>	C <sub>5</sub>	392.4	123.0 (H $\beta$ )	1.443
		392.4	-48.0 (H $\alpha$ )	2.364
C <sub>5</sub> =C <sub>6</sub>	C <sub>6</sub>	534.0	-43.0 (H $\alpha$ )	3.097
		534.0	168.0 (H $\beta$ )	1.960
thymine (with N-CH <sub>3</sub> )				
C <sub>2</sub> =O <sub>2</sub>	O <sub>2</sub>	394.3	24.0 (H $\beta$ )	1.986
			23.0 (H <sub>c5methyl</sub> )	1.991
			28.0 (H <sub>c5methyl</sub> )	1.964
C <sub>4</sub> =O <sub>4</sub>	O <sub>4</sub>	192.1	10.0 (H $\beta_{\text{methyl}}$ )	0.977
			-10.0 (H $\beta_{\text{methyl}}$ )	1.084
			-37.0 (H $\beta_{\text{N}}$ )	1.230
C <sub>5</sub> =C <sub>6</sub>	C <sub>5</sub>	459.2	-51.0 (H $\alpha$ )	2.738
C <sub>5</sub> =C <sub>6</sub>	C <sub>6</sub>	374.0	97.0 (H $\beta$ )	1.484
			96.0 (H $\beta_{\text{methyl}}$ )	1.489
			124.0 (H $\beta_{\text{methyl}}$ )	1.339
uracil (with N-CH <sub>3</sub> )				
C <sub>2</sub> =O <sub>2</sub>	O <sub>2</sub>	401.0	20.0 (H $\beta$ )	2.043
			-12.0 (H <sub>c5</sub> )	2.216
C <sub>4</sub> =O <sub>4</sub>	O <sub>4</sub>	197.0	11.0 (H $\beta$ )	0.997
			-37.0 (H $\beta_{\text{N}}$ )	1.256
C <sub>5</sub> =C <sub>6</sub>	C <sub>5</sub>	374.0	-52.0 (H $\alpha$ )	2.287
			113.0 (H $\beta$ )	1.398
C <sub>5</sub> =C <sub>6</sub>	C <sub>6</sub>	504.9	-51.0 (H $\alpha$ )	2.984
			157.0 (H $\beta$ )	1.863

lated,  $|\Delta M| = 1$ , resonances from the ab initio DFT methods. Because powder samples were used for these experiments, it is the perpendicular component of the axially anisotropic hyperfine tensor,  $A_\zeta$ , that is expected to show the highest intensity peak in the composite powder spectrum. Therefore the predicted level crossing resonance fields that are used for the following correlations are those of  $A_\zeta$ . The values that provided a linear correlation are shown in Figure 5. Those experimental resonances that did not fit this correlation were then plotted against the closest calculated resonances for the  $|\Delta M| = 0$  transitions, and were found to give the correlation given in Figure 6. Three resonances that did not fit either of these but formed a separate correlation with the  $|\Delta M| = 1$  resonances for O-Mu species from the ab initio DFT methods are shown in Figure 7.

It is interesting to find slightly different correlations depending on the atom to which the muon is attached as well as the type of resonance,  $|\Delta M| = 0$  or 1. Ab initio DFT calculations that are used in the present work predict properties of the electronic and vibrational ground states of the molecules. The correlations are obtained by using 300 K experimental data, and therefore the temperature effects on the hyperfine parameters discussed in general detail are of relevance to this case, Table 1. Of particular importance are the different orientations of the X-Mu bond with respect to the p-orbital on the adjacent atom containing the unpaired electron, in the ground-state structure. In the case of the C-Mu bonds formed from muonium addition to simple C=C double bonds it is an eclipsed configuration

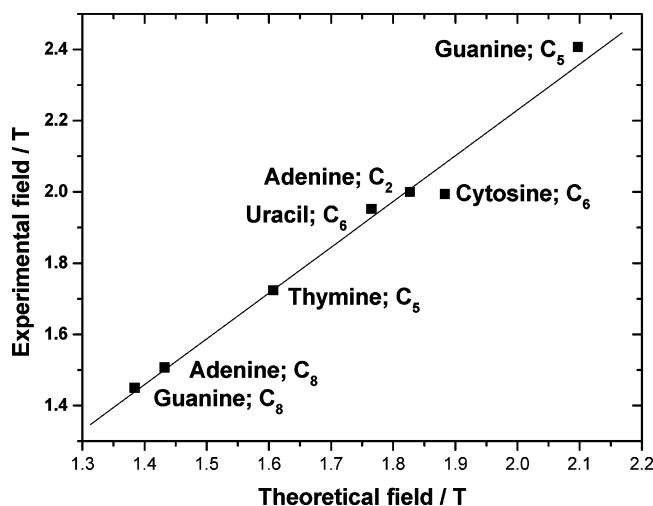


**Figure 5.** Correlation of DFT calculations with experimental data at 300 K for the  $|\Delta M| = 1$  resonance features for muon-carbon adducts of the nucleic acid bases. The linear correlation is  $B_{\text{expt}} = -0.3412 + 1.2857B_{\text{theory}}$ .

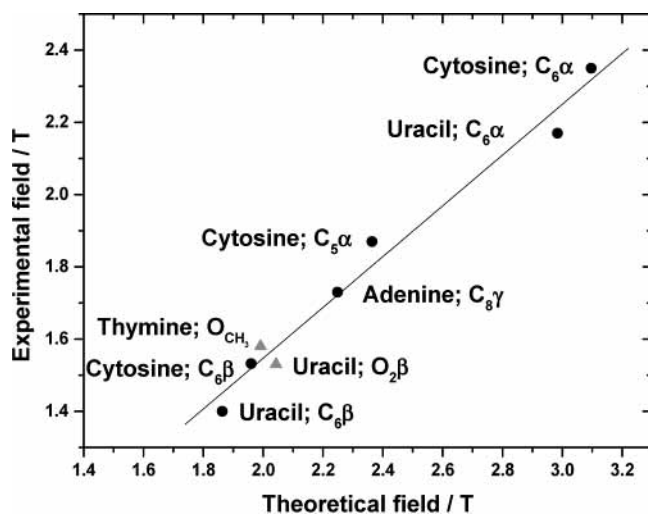


**Figure 6.** Correlation of DFT calculations with experimental data at 300 K for the  $|\Delta M| = 0$  resonance features for C-Mu and O-Mu adducts of the nucleic acid bases. The linear correlation is  $B_{\text{expt}} = 0.1414 + 0.7029B_{\text{theory}}$ .

between these two entities that has the lowest energy. This is the opposite to what is found in the case of C-H bonds and the reason for this difference is shown to be due to the difference in the zero-point energy of the X-Mu bond vibrations.<sup>14</sup> In contrast an O-Mu bond that results from muonium addition to a C=O group tends to have the O-Mu bond orthogonal to the  $\pi$ -orbital containing the unpaired electron.<sup>15,16</sup> This therefore will give rise to an increase in the hyperfine coupling with rise in temperature, a reflection of the increased amplitude of motion of the muon away from the position of orthogonality to the latter  $\pi$ -orbital. It is therefore reasonable to expect different correlations depending on the X atom as well as the type of transition.

The existence of these linear correlations provides an easy method of scaling of all the ab initio DFT hyperfine coupling parameters. The final scaled hyperfine couplings for all observed radicals are given in Table 5.

Within beamtime limitations, it was also possible to run ALC- $\mu$ SR of a powder sample of herring testes dsDNA. It is interesting to compare this spectrum with those obtained with the individual bases. Figure 8 shows such a comparison with all the observed and assigned radical resonances for the bases

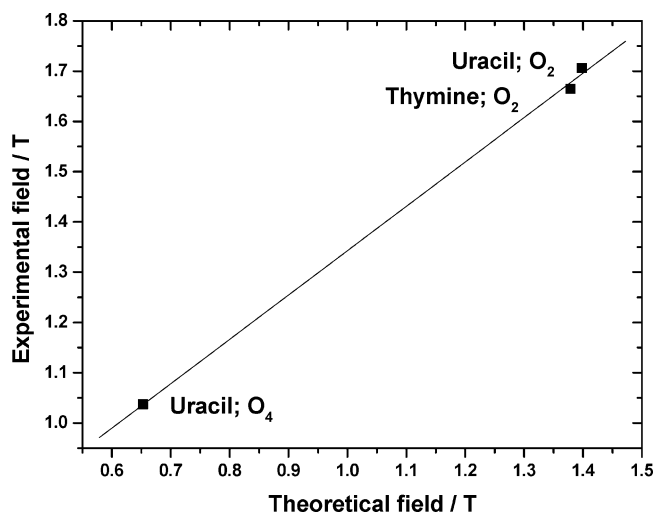


**Figure 7.** Correlation of DFT calculations with experimental data at 300 K for the  $|\Delta M| = 1$  resonance features for O-Mu adducts of thymine and uracil. The linear correlation is  $B_{\text{expt}} = 0.4605 + 0.8824B_{\text{theory}}$ .

**TABLE 5: Comparison of Theoretical and Experimental Hyperfine Couplings for the Muoniated Radicals of Nucleic Acid Bases That Are Identified during This Investigation**

unsaturated center	muon addition site and {proton site}	theoretical (DFT) $A_{\mu}/\text{MHz}$ and $\{A_p/\text{MHz}\}$	exptl $A_{\mu}/\text{MHz}$ and $\{A_p/\text{MHz}\}$ values
		adenine	
$C_8=N_7$	$C_8$	404	410.4
	$\{C_8H_{\gamma}\}$	$\{-15\}$	$\{87.4\}$
	$C_2$	516	544.6
		cytosine	
$C_5=C_6$	$C_5$	392	397 <sup>a</sup>
	$\{H_{\alpha}\}$	$\{-48\}$	$\{48\}$ <sup>a</sup>
	$C_6$	534	543
$C_5=C_6$	$\{H_{\alpha}\}$	$\{-43\}$	$\{104.3\}$
	$\{H_{\beta}\}$	$\{168\}$	$\{256.5\}$
			guanine
$C_8=N_7$	$C_8$	392	394.9
	$C_5=C_4$	580	655.5
		thymine	
$C_2=O_2$	$O_2$ (39.5°)	394	453.4
	$\{H_{\beta}\}$	$\{24\}$	$\{158.1\}$
$C_5=C_6$	$C_5$	459	469.5
		uracil	
$C_2=O_2$	$O_2$ (30.2°)	401	464.6
	$\{H_{\beta}\}$	$\{20\}$	$\{178.6\}$
$C_4=O_4$	$O_4$ (9.0°)	197	282.4
$C_5=C_6$	$C_6$	503	531.6
	$\{H_{\alpha}\}$	$\{-51\}$	$\{126.4\}$
	$\{H_{\beta}\}$	$\{157\}$	$\{269.7\}$

<sup>a</sup> ALC of the cytosine  $C_5$ -Mu radical was not experimentally observed, but estimated by using the linear correlations, and used to estimate the  $A_p$  value.

indicated as a stick diagram. It is immediately apparent that the signals from the dsDNA sample cover all the signals observed with the bases, but with some field shifts. However, the dsDNA spectrum is clearly not the simple sum of the spectra of the bases alone, showing additional polarization losses to both the higher and lower fields. Figure 8 also shows the calculated resonances for those radicals that were calculated by the DFT methods but not experimentally observed in this study with the pure bases, as black squares among the stick diagram. The field values for these resonances can be easily calculated

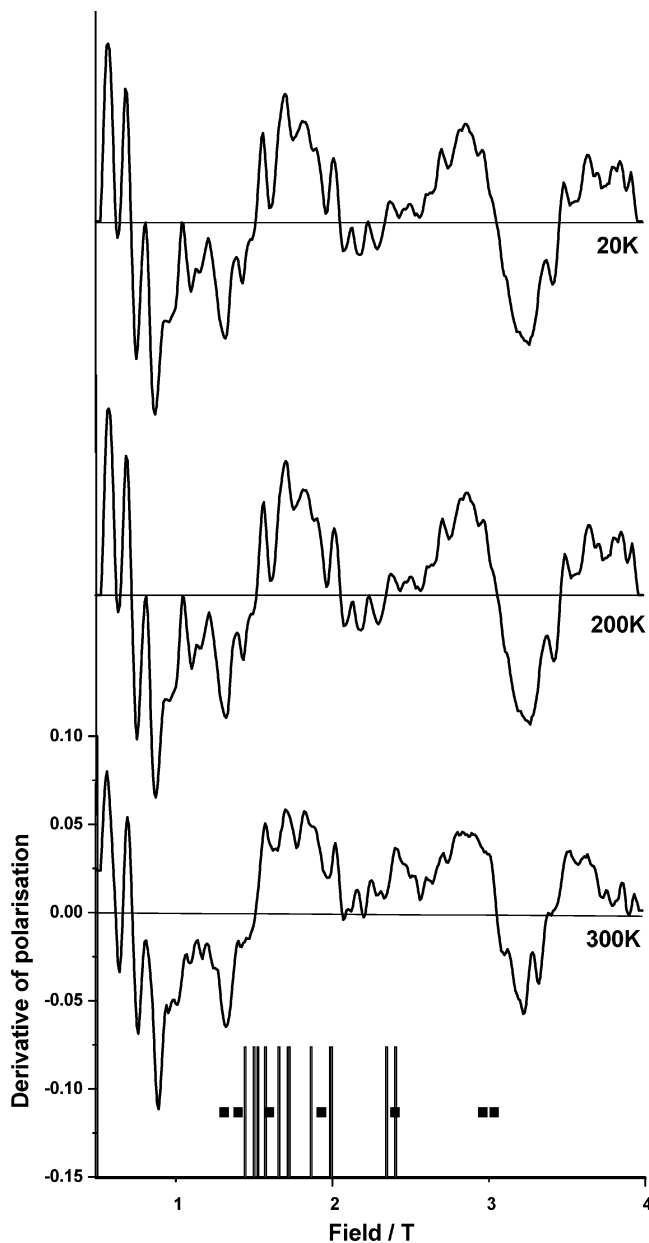


**Figure 8.** The ALC- $\mu$ SR spectra of dsDNA (Herring testes). The resonance signals observed and assigned for the different bases are indicated as a stick diagram for comparison. The predicted positions, using the DFT results and the linear correlations, of the other possible addition sites on the bases for which no experimental ALC signals were observed are indicated as dark squares.

by using the scaling factors reported here, together with the DFT predicted hyperfine interactions. These additional ALC field predictions in Tesla are, for adenine ( $C_6$ , 2.961;  $C_5$ , 2.403;  $C_4$ , 3.033), cytosine ( $C_2$ , 8.286;  $C_4$ , 6.541;  $C_5$ , 1.406), guanine ( $C_2$ , 1.605;  $C_4$ , 1.935), and thymine ( $C_2$ , 5.657;  $C_6$ , 1.317;  $O_4$ , 0.479). Figure 8 therefore shows clear evidence for muonium addition to these sites of the bases when presented as a part of the dsDNA molecule, a definite change from the behavior of the isolated bases.

The other ingredients of DNA in addition to the bases are the sugar phosphates. Spectra were run of polycrystalline samples of potassium phosphate and the sugar ribose. These two samples did not show any detectable resonances within the field range 0.001 to 5 T.

## Conclusion

This study has identified all primary radical species that resulted from muon implantation of the five nucleic acid bases. The ab initio DFT calculations were found to be invaluable in arriving at reliable assignments. Despite the large number of possible sites for muonium addition in these bases, there appears to be a clear preference only to a few sites. This is probably a reflection of the rates of addition.

Also reported here are the first confirmed experimental observations of unusually high hyperfine interactions predicted for O-Mu radicals of C=O groups. 410 and 418 MHz for the  $O_2$ -Mu adducts of thymine and uracil, respectively, and 150 MHz for the uracil  $O_4$ -Mu adduct. The cause of this appears to be due to the C=O group being a part of a ring system as well as the presence of a nitrogen atom on the adjacent ring site. To date the literature on such adducts reports a strong temperature dependence, with the hyperfine coupling increasing with an increase of the temperature.<sup>15,16</sup> This is due to the increased amplitude of the out-of-plane motion of the muon giving rise to an increase in the hyperconjugative interaction, which in turn gives rise to an increase in the unpaired electron density at the muon. All these radicals have structures with the muon situated in the nodal plane of the  $\pi$ -orbital containing the unpaired electron, and hence a very low hyperfine interaction at low temperature. The estimated values of the angle made by the O-Mu bond with the nodal plane of the  $\pi$ -orbital containing the radical electron for such adducts encountered in the present study are indicated in Tables 3 and 5. The observed temperature dependencies of the hyperfine interactions of these radicals are given in Table 1. Only three O-Mu radicals were observed. The radicals, uracil  $O_2$ -Mu ( $30.2^\circ$ ) and thymine  $O_2$ -Mu ( $39.5^\circ$ ), in fact show decreases in the hyperfine interaction with a rise in temperature with only the radical uracil  $O_4$ -Mu ( $9.0^\circ$ ) with the very small angle showing an increase in the hyperfine interaction with a rise in temperature in good agreement with the above-mentioned mechanism of hyperconjugation.

The only other  $\mu$ SR of nucleic acid bases is that by Barnabas et al.,<sup>5</sup> reporting ALC measurements of aqueous solutions of uracil, 6-methyluracil, 2-thiouracil, and thymine. They report resonance fields of 1.68, 1.825, and 2.368 T and also show spectra with reasonable signals in the case of uracil. These solution state  $|\Delta M| = 0$  resonances show a good linear correlation with the observed resonances at 1.40, 1.53, and 2.17 T for the solid-state samples at 300 K, studied during the present investigation, which are also assigned to  $|\Delta M| = 0$  resonances with the use of the ab initio DFT results, Table 4 and Figure 6, thus providing a confirmation of the above results. However, our experiments did not reproduce the results for thymine solutions reported by Barnabas et al.<sup>5</sup> This may be because of the presence of significant residual anisotropy combined with slow dynamics in the solid state tending to strongly enhance the  $|\Delta M| = 1$  resonances relative to the  $|\Delta M| = 0$  resonances, entirely opposite to what is observed in the liquid and gas phases. Fast motional averaging of the anisotropy in the latter phases greatly reduces the intensity of the  $|\Delta M| = 1$  resonances relative to the  $|\Delta M| = 0$  resonances. The suppression of  $|\Delta M| = 0$  resonances in the presence of strong hyperfine anisotropy has been simulated and discussed by Kreitzman and Roduner.<sup>17</sup> Significantly, the ab initio DFT methods used in the present study, which make very good predictions for all the other molecules, do not predict the hyperfine frequencies assigned by Barnabas et al.<sup>5</sup> This may be a consequence of the solubility problems encountered and stated by the former workers,<sup>5</sup> which

is likely to have caused difficulties, specially in the recognition of the weak features.

ALC- $\mu$ SR spectra of a powdered dsDNA sample show that the DNA spectra are definitely not a simple sum of the spectra of the bases. There are clear polarization losses in the former spectra to the higher and lower sides of all the features accountable for the isolated bases. Further, some of these additional features are readily accounted for by theoretical predictions of hyperfine parameters for the other possible sites on the bases that are not observed in the present investigation, assuming some shifts of the resonance field values. These observations suggest that the muonium addition rates to the nucleic acid bases are very dependent on their surroundings.

It may also be that the ionic phosphate that was used was not an appropriate model for DNA, and hence sugar phosphates themselves need investigation, to account for the extra features not fully accountable by the addition sites on the bases. Experiments to distinguish these possibilities with muon implantation of nucleosides and nucleotides are now planned. These experiments will be shadowed by ab initio calculations to track the changes that eventually occur on the way to the dsDNA structure.

**Acknowledgment.** We thank the Paul Scherrer Institute, Villigen, Switzerland for the muon facilities and the EPSRC for funding the project and a studentship to P.L.H., and the BBSRC for funding V.S.O.

#### References and Notes

(1) *ISIS Experimental Reports*; Rutherford Appleton Laboratory, RB No. 12143, 2001.

(2) Torikai, E.; Nagamine, K.; Pratt, F. L.; Watanabe, I.; Ikedo, Y.; Urabe, H.; Grimm, H. *Hyperfine Interact.* **2001**, 138, 509.

(3) See, for example: Pratt, F. L.; Blundell, S. J.; Hayes, W.; Nagamine, K.; Ishida, K.; Monkman, A. P. *Phys. Rev. Lett.* **1997**, 79, 2855.

(4) For details of ALC- $\mu$ SR spectroscopy, see, for example: Roduner, E. *Chem. Soc. Rev.* **1993**, 22, 337. *Muon Science; Muons in Physics, Chemistry and Materials*; Lee, S. L., Kilcoyne, S. H., Cywinski, R., Eds.; NATO Advanced Study Institute, 1998.

(5) Barnabas, M. V.; Venkateswaren, K.; Stadbauer, J. M.; Wu, Z.; Walker, D. C. *J. Phys. Chem.* **1991**, 95, 10204.

(6) Oganessian, V. S.; Hubbard, P. L.; Butt, J. N.; Jayasooriya, U. A. *Physica B* **2003**, 326, 25.

(7) (a) Baerends, E. J.; Ellis, D. E.; Ros, P. *Chem. Phys.* 1973, 2, 41. (b) Versluis, L.; Ziegler, T. *J. Chem. Phys.* **1988**, 88, 322. (c) Velde, G. te.; Baerends, E. J. *J. Comput. Phys.* **1992**, 99, 84. (d) Fonseca Guerra, C.; Snijders, J. G.; Velde, G. te.; Baerends, E. J. *Theor. Chem. Acc.* **1998**, 99, 391.

(8) Vosko, S. H.; Wilk, L.; Nusair, M. *Can. J. Phys.* **1980**, 58, 1200.

(9) Becke, A. D. *J. Chem. Phys.* **1986**, 84, 4524.

(10) Perdew, J. P.; Chevary, J. A.; Vosko, S. H.; Jackson, K. A.; Pederson, M. R.; Singh, D. J.; Fiolhais, C. *Phys. Rev. A* **1992**, 46, 6671.

(11) Versluis, L.; Ziegler, T. *J. Chem. Phys.* **1988**, 322, 88.

(12) Woo, T. K.; Cavallo, L.; Ziegler, T. *Theor. Chem. Acc.* **1998**, 100, 307.

(13) Heming, M.; Roduner, E.; Patterson, B. D.; Odermatt, W.; Schneider, J.; Baumeler, H.; Keller, H. *Chem. Phys. Lett.* **1986**, 128, 100.

(14) Claxton, T. A.; Graham, A. M. *J. Chem. Soc., Faraday Trans. 2* **1987**, 83, 2307.

(15) Macrae, R. M.; Rhodes, C. J.; Nishiyama, K.; Nagamine, K. *Chem. Phys. Lett.* **1996**, 259, 103. Macrae, R. M.; Briere, T. M. *Hyperfine Interact.* **1997**, 106, 169. Rhodes, C. J.; Reid, I. D.; Macrae, R. M. *Chem. Commun.* **1999**, 2157.

(16) Stride, J. A.; Jayasooriya, U. A.; Reid, I. D. *J. Phys. Chem.* **2002**, 106, 244.

(17) Kreitzman, S. R.; Roduner, E. *Chem. Phys.* **1995**, 192, 18.